Road Classification Using Built-In Self-Scaling Method of Bayesian Regression

Ai Hui Tan[a,*], Mathias Foo[b,1] and Duu Sheng Ong[c]

[a] Faculty of Engineering, Multimedia University, 63100 Cyberjaya, Malaysia; Email: htai@mmu.edu.my.

[b] School of Mechanical, Aerospace and Automotive Engineering, Coventry University, Coventry, CV1 5FB, United Kingdom; Email: mathias.foo@coventry.ac.uk.

[c] Faculty of Engineering, Multimedia University, 63100 Cyberjaya, Malaysia; Email: dsong@mmu.edu.my.

[*] Corresponding author

Abstract

This paper proposes the use of the built-in self-scaling (BS) method for ISO classification of road roughness. The technique employs the transfer function between the vehicle body acceleration as input and the suspension travel as output. This transfer function has a nonzero dc gain, which is important for application of the BS method. Frequency response magnitude patterns corresponding to this transfer function are estimated via Bayesian regression, capitalizing on the inherent properties of the BS method where the prior dc gain is incorporated into the formulation. This strategy leads to high classification accuracy. The proposed approach requires only low-cost sensors. It possesses a short detection time of 0.5s and a short training time of 5s for each road class. The method is model-free and does not require recalibration when the load carried by the vehicle changes. Additionally, it is capable of handling varying vehicle velocity and is effective for both passive and active suspensions. A laboratory-scale experiment shows that the proposed technique increases the percentage of correct classification by an average of 34% in the case of constant road profiles, compared with a state-of-the-art method using augmented Kalman filtering. A corresponding value of 24% is achieved for a varying road profile. The significant improvement in the accuracy of road classification is impactful as it will enable controller design for suspension systems to be enhanced resulting in more comfortable ride and higher vehicle stability.

Keywords: Bayesian regression; impulse response estimation; road classification; road roughness; vehicle suspension

[1] Present address: School of Engineering, University of Warwick, Coventry, CV4 7AL, United Kingdom; Email: M.Foo@warwick.ac.uk.

1. Introduction

Vehicle suspension is an important means for reducing unwanted vibrations caused by road roughness. Vertical displacements of the road can cause passenger discomfort and stability issues if the suspension system is not designed well. In particular, vehicle suspension system functions to improve primary ride comfort (i.e., in relation to the vehicle body motion sensed by the passengers) and to improve road handling (i.e., to ensure sufficient frictional forces exist between the road surface and the tires for the vehicle to be stable).

Road classification is useful in the context of vehicle suspension as the information can be utilized for automated adjustments of the suspension control parameters. For this purpose, it is advantageous if changes in the road roughness are detected quickly using as few low-cost sensors as possible. Many techniques are currently available for road classification. Some of these require costly equipment, such as ground-penetrating radars [1], profilographs [2] and laser profilometers [3]. Approaches employing Fourier transform (FT) are recommended in [4, 5]. These necessitate an accurate transfer function between the road displacement and either the vehicle body acceleration or the tire acceleration. The use of time-frequency feature, spatial-frequency feature and fast wavelet transform features along with a model of the vehicle dynamics is investigated in [6], where a precise dynamic model is crucial for accurate estimation. In [7], a combinatorial optimization technique is applied to determine the road profile based on accelerometer measurements. While only low-cost sensors are used, the method requires a long computation time.

In [8], a probabilistic neural network classifier is employed, where 29 features from both time and frequency domains are proposed for use in classification. This large number of features will lead to a significant increase in computation time. Conversely, reducing the number of features may cause performance deterioration. A deep neural network approach is proposed in [9], where the unsupervised feature learning is used. However, the time needed to train the neural network remains rather long. In [10], the authors make use of both longitudinal motion and vertical dynamics of the vehicle for road classification, where an integrated nonlinear model is developed and a combination of nonlinear Lipschitz observer and a modified super-twisting algorithm observer is employed for estimation of road profile and tire road friction.

A popular method for road classification is Kalman filtering (KF), which also represents the current state-of-the-art. KF is utilized in [11] where measurements of the wheel stroke (suspension deflection), acceleration of the sprung mass and acceleration of the unsprung mass are used along with a quarter-car model. Simultaneous estimation of state and input (unknown road roughness) using KF is performed in [12]. The augmented KF is applied in [13], where one of the aims is to process, in an off-line manner, large volumes of measurement data already collected. The augmented KF adds the road excitation to the state vector, resulting in an augmented state vector. The technique uses a model of reasonable complexity. Whether a simple model is sufficient depends on the particular suspension system. Model construction and accurate parameter identification are necessary for the KF method to work well. Additionally, noise covariances need to be selected; this requires knowledge about noise properties.

Despite the availability of many methods for road classification, there remains a gap for one that is model-free and requires very short training times. To this end, the current work proposes to tackle the issue using a Bayesian regression method, namely the built-in self-scaling (BS) method [14]. The classification is achieved due to the inherent characteristics of the BS formulation, which incorporates a dc gain term and reduces estimation variance at the expense of a bias. The proposed method utilizes the transfer function between the sprung mass (vehicle body) acceleration as input and the suspension travel as output in order to make use of the dc gain term.

The main contributions of this paper are as follows:

(i) A method for road classification is proposed using the BS technique. This technique has the advantages of requiring only low-cost sensors, being capable of detecting road class changes in a very short time of 0.5s, having a training time of only 5s per road class and being completely model-free. It remains effective without the need for recalibration when the load carried by the vehicle changes.

(ii) A new concept of performing classification using a Bayesian regression technique. Traditionally, in the field of machine learning, Bayesian regression and Bayesian classification are well separated [15].

(iii) A detailed case study using a real laboratory-scale experiment setup, where the proposed technique is compared with four other methods, namely the direct FT, least squares (LS), augmented KF and standard Bayesian kernel-based (KB) methods in both cases of passive and active suspensions. It should be pointed out that many of the previous works in road classification are entirely simulation based, for example [7–9].

The rest of the paper is organized as follows. Section 2 gives an overview of the quarter-car model and defines the problem statement. The proposed method is explained in

Section 3. A case study is discussed in Section 4, where detailed performance comparison with four other approaches is made. Finally, concluding remarks are given in Section 5.

2. Quarter-Car Model for Suspension System and Problem Statement

A quarter-car model for suspension system is chosen in the current work as it is widely accepted in the field of suspension control [8] and is the most frequently used model for ride comfort analysis [16]. It is also known that suspensions at different wheels are relatively independent [13] thus allowing wide applicability of the quarter-car model for suspension system.

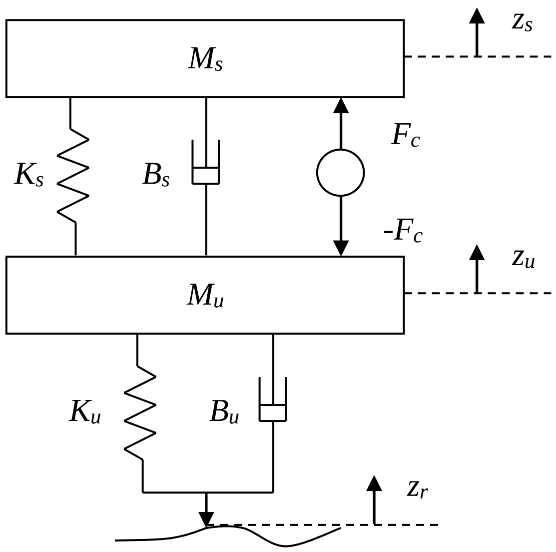

Fig. 1. Quarter-car model for suspension system.

A typical quarter-car model for suspension system is shown in Fig. 1, where M_s and M_u denote the sprung mass (vehicle body) and unsprung mass (tire), respectively. K_s and K_u denote the suspension stiffness and tire stiffness, respectively. B_s and B_u represent the suspension damping coefficient and tire damping coefficient, respectively. F_c is the force provided to the system when the system is operating in closed loop, under active suspension. When operating in open loop, $F_c = 0$. The road excitation is given by z_r, whereas the displacements of the sprung mass and unsprung mass from their static (nominal) positions are denoted by z_s and z_u, respectively.

If the components in the suspension system are assumed to be linear, the system can be modeled as two coupled second order linear systems, described by

$$M_u \ddot{z}_u = -B_s(\dot{z}_u - \dot{z}_s) + B_u(\dot{z}_r - \dot{z}_u) - K_s(z_u - z_s) + K_u(z_r - z_u) - F_c, \quad (1)$$

$$M_s \ddot{z}_s = B_s(\dot{z}_u - \dot{z}_s) + K_s(z_u - z_s) + F_c. \quad (2)$$

However, in practice, suspension systems are rarely very nearly linear. There may be nonlinearities in the springs and dampers [17]. Linear parameter-varying (LPV) models have been applied to model semi-active dampers in [18]. They have been employed to model nonlinear springs and dampers in [19]. In [20], the sprung mass is treated as an uncertain and time-varying scheduling parameter of an LPV model used for controller design.

The problem statement considered in this study is now formally stated as follows. It is required to classify road roughness according to the ISO road classes [21] using only low-cost sensors. The ISO road classification presents a standardized way of defining the roughness of a road. There are eight classes – A, B, C, D, E, F, G and H, ordered according to an increasing level of roughness. Details of the ISO road profiles and a review on research conducted using these profiles are given in [22]. The classification accuracy, defined by the ratio of the number of road segments correctly classified to the total number of segments, is to be maximized. A short detection time and a short training time are added advantages. Considering the nonlinearities in a real suspension system, the requirement for prior knowledge of system parameters should be avoided as far as possible.

3. Road Classification using BS Method

3.1 Overview of BS Method

In the Bayesian estimation framework for impulse response estimation, the system is described by

$$y_k = \sum_{i=0}^{k} u_{k-i} g_i + \varepsilon_k \quad (3)$$

where u_k, y_k, g_k and ε_k are the input, output, impulse response and measurement noise, respectively, at discrete time index k. The system output and the impulse response of length n are both treated as Gaussian random variables. In the case of short data record for estimation, the impulse response length n can be taken equal to the length of the data segment N. The impulse response $\mathbf{g} = [g_0 \quad g_1 \quad \dots \quad g_{n-1}]^T$ has a probability distribution $\mathbf{g} \sim \mathcal{N}(\mathbf{0}_n, \mathbf{K})$, where $\mathcal{N}$ denotes the normal (Gaussian) distribution, $\mathbf{0}_n$ is the n-dimensional zero column vector and $\mathbf{K} \in \Re^{n \times n}$ is the positive definite prior covariance matrix referred to as the kernel.

Let $\mathbf{y} = [y_0 \quad y_1 \quad \dots \quad y_{N-1}]^T$ and $\mathbf{U} = \begin{bmatrix} u_0 & 0 & 0 & \dots & 0 \\ u_1 & u_0 & 0 & & 0 \\ \vdots & \vdots & \ddots & & \vdots \\ u_{N-2} & u_{N-3} & \dots & & u_{N-n-1} \\ u_{N-1} & u_{N-2} & \dots & \dots & u_{N-n} \end{bmatrix}$. Then the *a priori* distribution is

$$\begin{bmatrix} \mathbf{y} \\ \mathbf{g} \end{bmatrix} \sim \mathcal{N}\left(\begin{bmatrix} \mathbf{0}_N \\ \mathbf{0}_n \end{bmatrix}, \begin{bmatrix} \mathbf{UKU}^T + \sigma^2 \mathbf{I}_N & \mathbf{UK} \\ \mathbf{KU}^T & \mathbf{K} \end{bmatrix} \right) \tag{4}$$

where σ^2 denotes the variance of the zero-mean output Gaussian noise. The assumption of Gaussian noise is important as the conditioning of jointly Gaussian random variables (in this case, $\mathbf{g}$ and $\mathbf{y}$) is a key element in kernel-based estimation methods [15]. This allows the conditional distribution of $\mathbf{g}$ given $\mathbf{y}$ to be formulated based on Bayes' rule, giving the posterior distribution. The posterior distribution of $\mathbf{g}$ is given by $\mathbf{g}|\mathbf{y} \sim \mathcal{N}(\hat{\mathbf{g}}, \hat{\mathbf{K}})$ [15] where

$$\hat{\mathbf{g}} = \frac{1}{\sigma^2} \hat{\mathbf{K}} \mathbf{U}^T \mathbf{y}\,, \; \hat{\mathbf{K}} = \left(\mathbf{K}^{-1} + \frac{1}{\sigma^2} \mathbf{U}^T \mathbf{U} \right)^{-1}. \tag{5}$$

Note that $\hat{\mathbf{g}}$ is defined as the estimated impulse response. The use of Eq. (5) for the estimation of impulse response is referred to as the standard KB method. The Bayesian estimation framework offers important advantages such as smaller total mean squared error due to a much lower variance at the expense of a slight bias, improved numerical conditioning and the ability to perform estimation using short data records.

The BS technique offers significant improvement over the standard KB method via incorporation of a dc gain term. It is shown in [14] that the BS method results in higher estimation accuracy compared to the standard KB method as well as another Bayesian estimation technique, which first estimates the step response by dividing it into steady-state and residual constituents and then constructs the impulse response of the system [23].

In the BS approach, the dc gain of the system is modeled by $s_\infty \sim \mathcal{N}(s_\infty^*, \sigma_\infty^2)$ where both s_∞^* and σ_∞^2 are known *a priori*. The actual value of the dc gain s_∞ is defined by $s_\infty = \sum_{k=0}^{n-1} g_k$. Incorporating the dc gain term requires that $\mathbf{y}$ and $\mathbf{U}$ be modified to

$$\tilde{\mathbf{y}} = \begin{bmatrix} y_0 & y_1 & \dots & y_{N-2} & \eta s_\infty^* \end{bmatrix}^T \text{ and } \tilde{\mathbf{U}} = \begin{bmatrix} u_0 & 0 & 0 & \dots & 0 \\ u_1 & u_0 & 0 & & 0 \\ \vdots & \vdots & \ddots & & \vdots \\ u_{N-2} & u_{N-3} & \dots & & u_{N-n-1} \\ \eta & \eta & \eta & \dots & \eta \end{bmatrix}, \text{ with } \eta = \sqrt{\sigma^2 / \sigma_\infty^2}.$$

The posterior distribution for the BS method is given by $\mathbf{g} | \tilde{\mathbf{y}} \sim \mathcal{N}(\hat{\mathbf{g}}, \hat{\mathbf{K}})$ where

$$\hat{\mathbf{g}} = \frac{1}{\sigma^2} \hat{\mathbf{K}} \tilde{\mathbf{U}}^T \tilde{\mathbf{y}}, \ \hat{\mathbf{K}} = \left(\mathbf{K}^{-1} + \frac{1}{\sigma^2} \tilde{\mathbf{U}}^T \tilde{\mathbf{U}} \right)^{-1}. \tag{6}$$

3.2 Derivation of Transfer Function

Commonly used variables for vehicle suspension system for the evaluation of the effects of vibration caused by the road are the suspension travel and the body acceleration. Suspension travel is the relative displacement between the vehicle body and the tire and must be constrained within an allowable workspace. Body acceleration is a measure of ride comfort. The transfer function between suspension travel and road velocity in open loop can be derived using Eq. (1) and Eq. (2). It is given by

$$\frac{Z_s(s) - Z_u(s)}{sZ_r(s)} = \frac{-sM_s(sB_u + K_u)}{\begin{bmatrix} M_sM_us^4 + (M_sB_s + M_sB_u + M_uB_s)s^3 + (M_sK_s + \\ M_sK_u + M_uK_s + B_sB_u)s^2 + (B_sK_u + B_uK_s)s + K_sK_u \end{bmatrix}}, \tag{7}$$

where Z_s, Z_u and Z_r are the Laplace transforms of z_s, z_u and z_r, respectively, and s is the Laplace variable. The transfer function between the body acceleration and road velocity is given by

$$\frac{s^2Z_s(s)}{sZ_r(s)} = \frac{s(B_sB_us^2 + (B_sK_u + B_uK_s)s + K_sK_u)}{\begin{bmatrix} M_sM_us^4 + (M_sB_s + M_sB_u + M_uB_s)s^3 + (M_sK_s + \\ M_sK_u + M_uK_s + B_sB_u)s^2 + (B_sK_u + B_uK_s)s + K_sK_u \end{bmatrix}}. \tag{8}$$

While these transfer functions are very useful, they both give a gain of zero at dc. Thus, they cannot be used with the BS method, as the BS method requires a nonzero dc gain.

In light of the above, the proposed method uses the transfer function between the body acceleration as input and the suspension travel as output. This transfer function is defined by

$$\frac{Z_s(s) - Z_u(s)}{s^2Z_s(s)} = \frac{-M_s(sB_u + K_u)}{B_sB_us^2 + (B_sK_u + B_uK_s)s + K_sK_u}. \tag{9}$$

Only the relative displacement between the body and the tire from the estimated (reference) relative position is required; the absolute displacement is not needed. Importantly, the dc gain magnitude is given by M_s / K_s. Note that the sprung mass M_s affects only the gain but not the dynamics (zeros and poles) of the transfer function. Since M_s is the parameter which is most subject to variation due to changes in the load, the invariance of the dynamics with respect to M_s is advantageous as no recalibration is needed when M_s changes. The change in the gain is effectively handled by fixing the prior dc gain in the BS method (see Remark 5 in Section 4.2 for an illustration of this point).

Note also that the denominator of Eq. (9) is a second order polynomial; this is in contrast with a fourth order polynomial in Eq. (7) and Eq. (8). In order words, the transfer function in Eq. (9) will have at most one resonant frequency (and that is if the system is underdamped), compared with two resonant frequencies in Eq. (7) and Eq. (8).

3.3 Novel Road Classification Method

A novel way of performing road classification using the BS technique will now be explained. The BS technique first results in the estimation of the system impulse response. On this point, note that only a handful of methods make use of impulse response characterization. Examples are described in [24, 25] where the impulse responses are utilized as a means to evaluate controller performance, and in [26] where they are applied to extract the modal parameters of a vehicle.

To apply Eq. (6), a kernel **K** is needed. Many different types of kernels are available in the literature. A simple kernel will suffice for this application. Examples are the tuned-correlated (TC) kernel where the (*p, q*)th element of the matrix is given by

$$\mathbf{K}_{p,q} = c\lambda^{\max(p,q)} \tag{10}$$

and the diagonal-correlated (DC) kernel which is defined by

$$\mathbf{K}_{p,q} = c\lambda^{(p+q)/2}\xi^{|p-q|} \tag{11}$$

with $c \geq 0$, $0 \leq \lambda \leq 1$ and $|\xi| \leq 1$ [27]. These kernels have only two and three hyperparameters, respectively, to optimize, making the tuning process as simple as possible. Tuning can be carried out using the Empirical Bayes method [28], which is a popular method for hyperparameter tuning.

The impulse responses are subsequently converted into the frequency domain to give frequency responses. The frequency response magnitude (FRM) patterns obtained will be different for different road classes, if the system has a nonlinearity which is amplitude-dependent. These FRM patterns are applied for classification. Since the objective here is to perform road classification and not to estimate accurate frequency responses, the following should be noted:

Remark 1: If the system under test is nonlinear, as would likely be the case for a suspension system, the posterior distribution for the BS method will correspond to the Bayesian estimate of the system's best linear approximation (BLA). The BLA is the linear model which gives the best fit to the system dynamics, in the least mean square sense. If the exact dynamic model of the system and the amplitude distribution of the input signal are available, the BLA can be derived theoretically, for example, making use of the input-output cross-correlation function [29]. However, the proposed approach does not require the theoretical BLA to be computed. More importantly, the FRM patterns of the BLAs for different road classes are distinguishable from one another. Hence, the nonlinear distortion in the system does not limit the application of the proposed technique.

Remark 2: It is well known that the TC kernel is unable to model resonances [30] due to it having a single pole. However, for the objective above, this kernel suffices.

Remark 3: Only the magnitude of the frequency response is used for classification. Hence, a positive dc gain term s_∞^* is recommended, even if the actual gain of the transfer function is negative. Based on observation, this will result in higher estimation accuracy, due to better conditioning of the problem.

To obtain the reference FRM patterns for each road class, several road segments (for example, 10 segments) are used and the reference FRM patterns for each class are computed by averaging across the number of segments. The reference FRM patterns are then applied by comparing the FRM of each road segment to be classified with the reference FRM patterns. The road is classified based on which of the reference FRM patterns is the closest to the segment being tested, according to

$$p_{\text{opt}} = \arg\min_p \left(\sum_k \left(\log_{10} \mathbf{X}(k) - \log_{10} \mathbf{R}_p(k) \right)^2 \right) \tag{12}$$

where p represents the road class (A, B, C, and so on) and p_{opt} is the estimated road class. $\mathbf{X}$ denotes the FRM of the segment under test, $\mathbf{R}_p$ denotes the FRM of the reference for road class p and k represents the harmonic number corresponding to the frequencies of interest.

Several interesting methods are available where the frequency analysis is performed in the spatial domain, after combining the information of the vehicle velocity and the system response, such as those described in [6, 31]. The key reason why the spatial domain is not used in the current work is because there is no accurate model being estimated by the proposed approach, which can transform the system response from the time domain into the spatial domain. The proposed technique is unique in the sense that it is model-free. Furthermore, performing the frequency analysis in the time domain allows the frequency range to focus on the range that is important for vehicle dynamics, i.e., covering the natural frequencies of the vehicle.

3.4 Handling of Varying Vehicle Velocity

Varying vehicle velocity is a very challenging problem for road classification. In [7, 8], an assumption of fixed velocity is applied. In [9], a quadratic velocity correction factor is utilized; this requires the coefficients of the correction factor to be tuned via extensive simulations for different velocities. The augmented KF proposed in [13] underestimates the road profile power spectral density (PSD) at high spatial frequencies when the vehicle velocity is high, and underestimates the PSD at low spatial frequencies when the vehicle velocity is low. This is due to certain spatial frequencies not generating sufficiently large responses from the vehicle at certain velocities. While approaches using detailed models of the vehicle can cope with varying velocity, such as that in [10], these lead to a different problem of possible model mismatches.

The BS method handles varying velocity in a simple manner based on the relationship between velocity and spatial frequency. To illustrate this, suppose that a vehicle travels at v ms^{-1} on a sinusoidal road with amplitude of 1m and a spatial frequency of 1 cycle/m. A second vehicle travels at av ms^{-1} on a different sinusoidal road with amplitude of 1m and a spatial frequency of $1/a$ cycle/m. Both vehicles will experience the same vertical forces exerted by the road, on the same time scale. In other words, a smoother road will feel rougher to a vehicle travelling at a higher velocity.

The BS technique can cater for different velocities by storing the FRM patterns for different velocities across the entire operating range of the vehicle. Since the velocity is a readily available measurement in a standard vehicle, the average velocity measured across a segment is supplied to the classification algorithm to enable the correct set of FRM patterns to be referred to for classification. With the length of the segment (and the corresponding time duration) being short, the velocity variation across an individual segment is expected to be small. In other words, even though it is well known that methods based on frequency response cannot deal directly with changing velocity, the BS method overcomes this by allowing the velocity to change from segment to segment and limiting the duration of an individual segment.

4. Case Study

4.1 Experiment Settings

The system used for experimentation is a suspension system from Quanser [32]. The test rig has a length of 30.5cm, a width of 30.5cm and a height of 61cm. It has a total weight of 15kg. The system consists of three masses that represent the road, body and tire, and which move along stainless steel shafts using linear bearings. The system utilizes a brushed dc motor connected to a belt-drive mechanism to simulate the road surface whereas a brushless dc motor is used to implement active suspension control. The system has limitations such that the maximum displacements of the road, body and tire are constrained to ±22mm, ±25.4mm and ±19mm, respectively, from their reference positions.

Five road profile signals were generated using multisine with amplitude spectra shaped according to the ISO road Classes A, B, C, D and E for frequency range between 0.2Hz to 200Hz. No signal power was applied for frequency below 0.2Hz due to the maximum displacement of the road being constrained to ±22mm from the reference position. No signal power was applied for frequency above 200Hz as this range is unimportant for suspension system analysis [22]. The range between 0.2Hz to 200Hz is also justified by the fact that it covers the natural frequencies of the system. The natural frequencies of a passenger car are typically 1-2Hz for the sprung mass and 10-15Hz for the unsprung mass [33]. A vehicle velocity of 18km/hr ($5ms^{-1}$) was applied in the conversion between spatial frequency and cyclic frequency. A low velocity was selected because the roads D and E are rather rough. (A faster vehicle will be considered in Section 4.4.) In the ISO classification, the road PSD is defined as a decreasing function of the spatial frequency. Note that vehicle velocity × spatial frequency = cyclic frequency. By fixing the range of interest of the cyclic frequency, the spatial frequency can be increased by decreasing the vehicle velocity. This reduces the road PSD and height of the road profile to satisfy the physical limitations of the Quanser system.

The sampling frequency was set to 500Hz. The road profile signals were generated as periodic signals with a period of 50,000 samples. Three periods of the suspension travel and body acceleration were measured after the system had reached steady-state. There were therefore 150,000 data points collected for each road profile. (A data point here is defined as a measurement of suspension travel and body acceleration at a sampling time instant.) It should be emphasized that the periodic property was not utilized in any of the methods used for performance comparison, except in the augmented KF method for the setting of noise covariances. The passive system operating in open loop was considered. (The active system operating in closed loop was tested later in Section 4.3.) The road profile PSD, as well as those of the body displacement and the tire displacement, is plotted in Fig. 2. The PSDs of the body displacement and the tire displacement are corrupted by a large amount of noise because the displacement signals are very small, due to the physical limitations of the Quanser system.

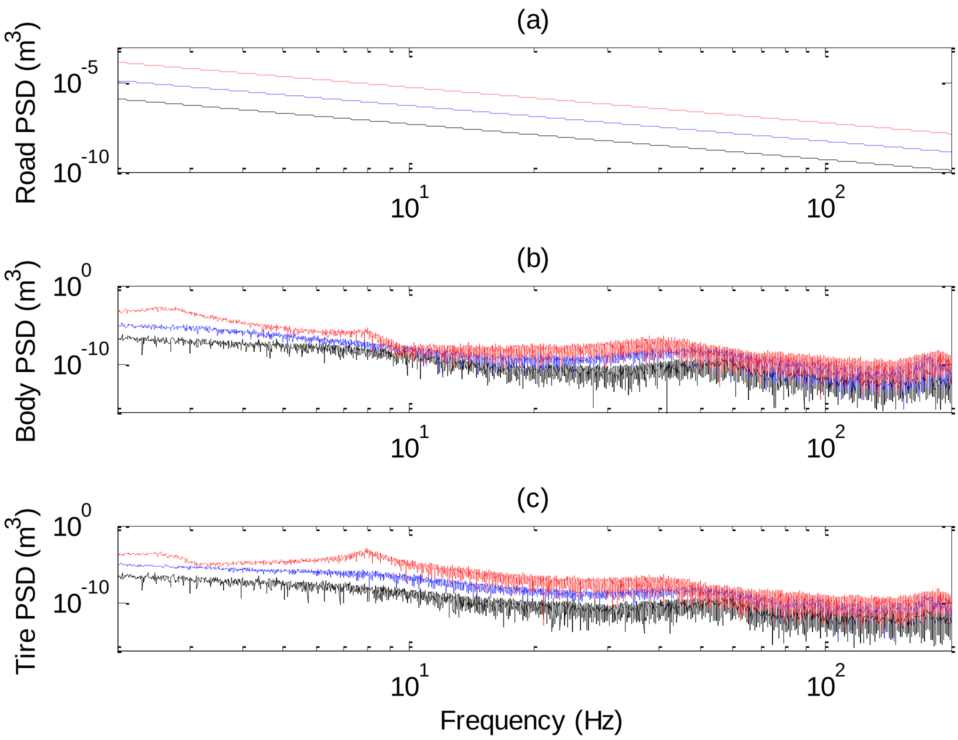

Fig. 2. Displacement PSDs of (a) road, (b) body and (c) tire. Black solid line: Class A; blue dashed line: Class C; red dashed-dotted line: Class E.

The FRMs obtained are shown in Fig. 3. In subplot (a), the FRMs were obtained directly from the data without any denoising. In subplot (b), three periods of data were averaged to form an averaged period before estimating the frequency responses and a lower frequency resolution was applied to improve the smoothness of the FRMs. Those corresponding to road profiles B and D are not plotted for the sake of visual clarity. Note that at most one resonant frequency appears, consistent with Eq. (9). It can be seen that the frequency responses change with road roughness and can thus be utilized for classification purposes. An important advantage of the non-parametric identification here is that no model needs to be constructed. This greatly minimizes the modeling effort required as it is not an easy task to construct a nonlinear or LPV model while a linear model is clearly insufficient for explaining the variation of the frequency responses with road roughness.

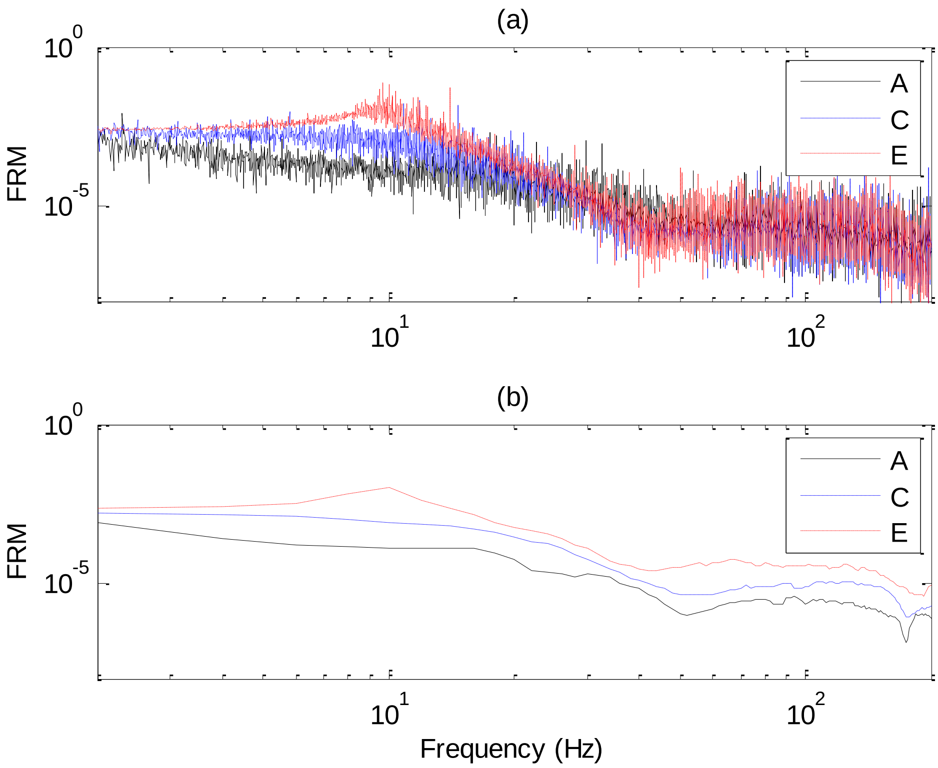

Fig. 3. FRMs of $\dfrac{Z_s(s)-Z_u(s)}{s^2 Z_s(s)}$ for different road profiles (a) without averaging and (b) with averaging.

4.2 Performance Comparison

Five methods, namely the direct FT, LS, augmented KF (denoted simply by KF), standard KB and BS techniques were applied to test the accuracy of road classification. For each road profile, the 150,000 data points were divided into 600 segments with 250 points each (N = 250). Each segment corresponds to a very short duration of 0.5s.

For each of the FT, LS, KB and BS methods and road profiles, the first 10 segments were used for generating the reference FRM pattern, while the remaining 590 segments were utilized for testing. Only frequencies between 2Hz and 20Hz, corresponding to harmonics 1 to 10 (k = 1 to 10 in Eq. (12)), were applied for classification because higher frequencies suffer more from the effects of noise. Based on our observations, all of these four approaches deteriorated when higher frequencies were considered.

The FT method takes the discrete FT of the output (suspension travel) divided by the discrete FT of the input (body acceleration). The application of a moving average filter for smoothening the frequency response was also studied but no improvement could be obtained; hence, the results reported here are those obtained without the moving average filter. The LS technique first estimates the impulse response of length N based on the finite impulse response model. The result is then converted into the frequency domain via discrete FT. There is little point in using an impulse response length shorter than N because the impulse response is not fully settled after 0.5s. Nevertheless, this does not affect the results as the classification is achieved based on comparison with the reference FRM patterns rather than with the frequency response of the actual system.

The KB technique was applied using a TC kernel. The kernel was tuned based on one segment of data, in this case arbitrarily chosen as the first segment for road profile Class A. Tuning was performed using the Empirical Bayes method resulting in $\mathbf{K}_{p,q} = 0.2946 \times 0.5996^{\max(p,q)}$. The value of σ^2 was set as 0.04 after several values were tested and this value gave rather robust performance. The same parameters were utilized for the BS method. All the segments of data points for the five road profiles were processed using Eq. (6) (or Eq. (5) for the KB method) applying the same kernel. The dc gain for the BS method was set to s_∞^* = 0.0027 using the nominal values of the suspension parameters, i.e., M_s = 2.45kg and K_s = 900Nm^{-1} provided by Quanser [32]. The value of σ_∞^2 was set of 7.29×10^{-8}, computed assuming that $\sigma_\infty = 0.1 s_\infty^*$. More comments on this will be given shortly.

The KF technique is rather different from the rest and represents the current state-of-the-art for road profile estimation. The augmented KF proposed in [13] was utilized. However, for good performance, the noise covariances need to be selected carefully. In the current paper, these matrices were tuned optimally through analysis of the noise properties, which is made possible due to three periods of data being collected. The periodic property of the road profile signal was employed to quantify the effects of noise, following the method described in [34, 35]. The regularization parameter was selected by testing several values and choosing the one that resulted in the highest classification accuracy. For fair comparison with the other approaches, the first 10 segments were applied for the tuning of the error covariance matrix. The classification was performed by comparing the variance of the estimated road profile with the reference variances of road Classes A to E and selecting the estimated road class based on the smallest difference between the variances according to

$$p_{\text{opt}} = \arg\min_{p} \left(\left|\operatorname{var}(\mathbf{u}_{\text{est}}) - \operatorname{var}(\mathbf{u}_{p})\right|\right) \tag{13}$$

where $\mathbf{u}_{\text{est}}$ denotes the estimated road profile of the segment under test and $\mathbf{u}_p$ denotes the actual road profile of the reference for road class p.

The results obtained are shown in Table 1. Note that the sum of each row is 590. The percentages of correct classification across all five road profiles are 49.1% for FT, 33.3% for LS, 52.2% for KF, 48.1% for KB and 86.1% for BS. The improvement achieved by the BS method is very significant. The detection time is 0.5s and the training time is 5s for each road class, for all five methods. It is also worth noting that the number of cases where a road segment was incorrectly classified more than one class away (such as road Class A being classified as C, D or E) are very low for the KF and BS techniques. The percentages are 12.3% for FT, 25.5% for LS, 0.44% for KF, 22.6% for KB and 0.64% for BS. This indicates that when incorrect classification occurs for the KF and BS techniques, the subsequent negative impact in terms of suspension control is less detrimental.

To understand the reason behind the improvement offered by the BS technique, the estimated FRM patterns for 10 segments of road Classes A and E are plotted in Figs. 4 and 5 for the FT and BS approaches, respectively. The FRM patterns for the FT method have overlap between those of Classes A and E, even at low frequencies, although the overlap is worse at high frequencies. This overlap makes classification difficult. This is also true for the LS and KB methods. (Based on Fig. 4, where the separation between the FRM A and E patterns is largest at 10Hz, the use of a single frequency at 10Hz for FT classification was also attempted, but the accuracy was only 33.9%.) However, the BS technique does not suffer from this problem for frequencies below 20Hz. The key to this is the use of the dc gain in the BS formulation enabling all the FRM patterns to start at almost the same value in addition to the lower variance in the FRM patterns due to the bias-variance trade-off common to Bayesian methods. This means that even if the FRM patterns corresponding to the FT and LS techniques were normalized to start at a fixed point, the higher variance would still result in the overlap of FRM patterns and subsequently poor classification accuracy.

Table 1. Classification results for various methods at 18km/hr ($5 ms^{-1}$). The bold values indicate correct classification.

Actual road class	Method	Number of occurrences of estimated road class				
		A	B	C	D	E
A	FT	**474**	107	8	1	0
	LS	**441**	71	68	5	5
	KF	**443**	144	3	0	0
	KB	**84**	65	314	127	0
	BS	**466**	122	2	0	0
B	FT	302	**204**	78	6	0
	LS	319	**96**	142	29	4
	KF	55	**490**	45	0	0
	KB	67	**49**	326	148	0
	BS	98	**460**	32	0	0
C	FT	138	94	**324**	19	15
	LS	44	16	**87**	176	267
	KF	0	0	**15**	565	10
	KB	71	36	**388**	95	0
	BS	0	5	**528**	57	0
D	FT	16	30	324	**42**	178
	LS	70	29	177	**220**	94
	KF	0	0	0	**1**	589
	KB	2	2	60	**422**	104
	BS	0	0	6	**559**	25
E	FT	1	0	149	36	**404**
	LS	47	14	170	221	**138**
	KF	0	0	0	0	**590**
	KB	0	0	4	111	**475**
	BS	12	4	1	46	**527**

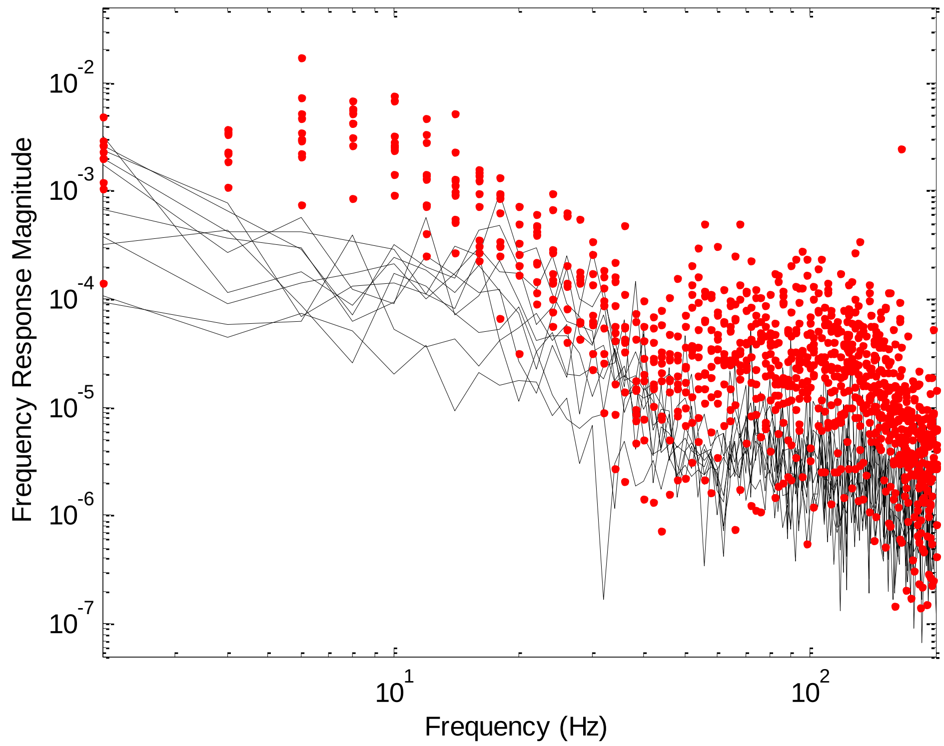

Fig. 4. FRM patterns for the FT method. Black solid lines: Class A; red dotted lines: Class E.

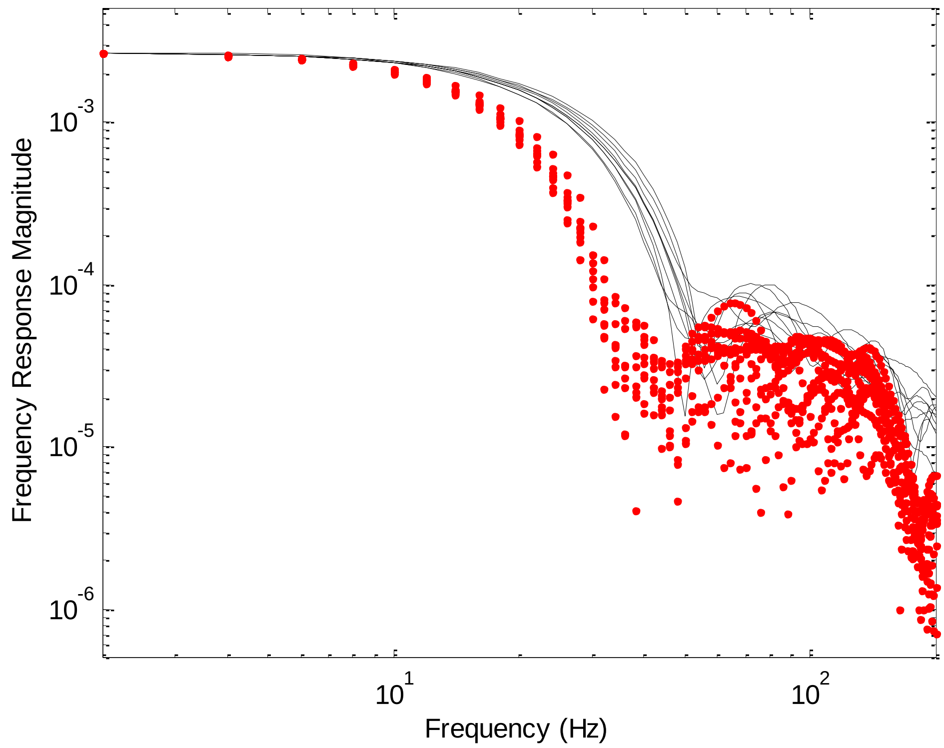

Fig. 5. FRM patterns for the BS method. Black solid lines: Class A; red dotted lines: Class E.

As for the KF technique, the classification accuracy depends very much on the regularization parameter and the actual road class. Changing the value of the regularization parameter would vary the accuracy for different road classes (the value was set to give overall highest accuracy in this work), showing that the effectiveness of this technique relies heavily on proper tuning of the parameters used. In contrast, the BS technique is much less sensitive to user-selection of parameter values.

Some further comments are in order, as follows:

Remark 4: The *a priori* value of s_∞^* in the BS technique is not very important. Indeed, when tested using a value of s_∞^* = 0.027, which is 10 times larger than the nominal value, a similar separation as in Fig. 5 was attained, although the dc value was incorrect. The accuracy is largely unaffected by the value of s_∞^* as long as the same value is used for generating the reference FRM patterns during training and for performing classification. The separation can be achieved provided σ_∞^2 is small compared to σ^2. The BS method is thus fit for the purpose for road classification, noting that it is not required to estimate the actual FRM. It can be seen from Fig. 5 that the resonance is not captured in the FRM patterns.

Remark 5: A test was conducted to investigate if classification will remain effective with changes in the sprung mass that is affected by the number of passengers and other loads. Keeping the same reference FRM patterns obtained with the original value of M_s, the value of M_s was increased by 30% (artificially though computer manipulation by adjusting the magnitude of the output signal) during the classification phase. No retuning was done and the *a priori* value of s_∞^* = 0.0027 remained unchanged throughout the test. The percentage of correct classification remained very high at 82.7%. The percentage of cases where a road segment was incorrectly classified more than one class away remained very low at 1.46%. Decreasing the value of M_s by 30% gave 89.0% accuracy with 0.31% of the segments incorrectly classified more than one class away. These results show that the proposed approach is very practical as it remains effective under variations in the sprung mass, without requiring recalibration.

Remark 6: Since the purpose is only to perform classification, an accurate value of σ^2 is not required in the KB and BS approaches. The estimation of the noise color is also not needed. Indeed, the input signal (body acceleration) is itself corrupted with noise but this does not require any special treatment. The fact that the input is also corrupted with noise implies that the noise affecting the transfer function is, in general, non-Gaussian. This does not affect the proposed use of the BS method for road classification since it is not necessary to accurately estimate the actual FRM.

Remark 7: The use of a different kernel was tested for the BS method. A popular kernel, besides the TC kernel applied earlier, is the DC kernel. Again, the kernel was tuned based on a single segment of data, now arbitrarily chosen as the first segment corresponding to road profile Class E. Tuning using Empirical Bayes led to $\mathbf{K}_{p,q} = 0.2385 \times 0.3724^{(p+q)/2} 0.8376^{|p-q|}$, with σ^2 remaining at 0.04. The accuracy was 84.8%. There was not a single case where a segment was incorrectly classified more than one class away. The effectiveness of the BS technique in this case remains even with a different kernel and a correspondingly different set of reference FRM patterns.

4.3 Extension to Active Suspension

To ensure that the proposed classification using the BS approach is practical, it must work also under active suspension (i.e., in closed loop). The suspension system from Quanser was implemented in a closed loop with a linear quadratic regulator (LQR) controller. The performance of the various methods is shown in Fig. 6. It can be seen that overall, the KF, KB and BS techniques attained an improvement from the open loop case, whereas the opposite was observed for the FT and LS techniques. The BS technique remains far superior to the other four methods. As a note, the fluctuations observed in the plots are due to the randomness of noise in the experiments.

It is interesting to highlight the large difference in classification accuracy for the KF method in the open loop and in the closed loop. In the latter case, the controller serves to reduce the difference between the dynamic responses of the system for different road classes, which is advantageous to the KF method. In contrast, the FT, LS, KB and BS techniques rely on the system exhibiting different responses for different road classes. In the present Quanser system, the differences are non-negligible (refer to Fig. 3). The system dynamics are highly complicated, where detailed modeling employing a linear model (using the periodic data) proved challenging. Even though the system is theoretically of fourth order, the dynamics could not be satisfactorily captured even with model orders as large as 10. This is foreseeable in practical systems. An important advantage of the BS approach is that no modeling is needed; it is model-free. The findings may indicate that the most suitable method for a particular system (KF or BS) would depend on the degree of nonlinearity or LPV behavior in the system. These methods can thus be viewed as complementary to each other, and both can find suitable applications in practice.

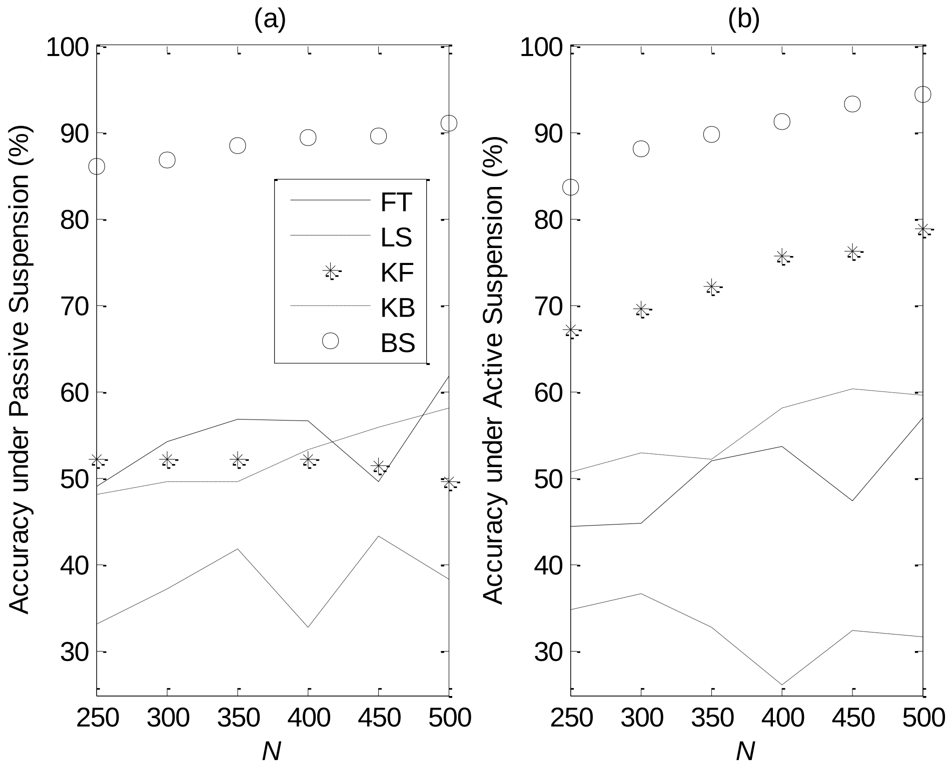

Fig. 6. Accuracy of various methods under (a) passive suspension (open loop) and (b) active suspension (closed loop).

Overall, the improvement in the accuracy for all five methods increases very slowly with N, although KF worsens slightly with N in the passive case and LS deteriorates slightly in the active case. Thus, it seems unnecessary to use a large N. For this particular system, at a sampling frequency of 500Hz, N = 250 can be considered ideal as it gives the first harmonic at 2Hz which is close to the natural frequency of the sprung mass. In other words, N = 250 gives as short as possible a detection time of 0.5s and yet is able to cover the resonant frequencies of the system.

A subsequent experiment was conducted to investigate the effectiveness of the various methods under a road profile with varying road class as shown in Fig. 7. The results for the active suspension case are depicted in Fig. 8. Those for the passive suspension case are similar and are thus not shown.

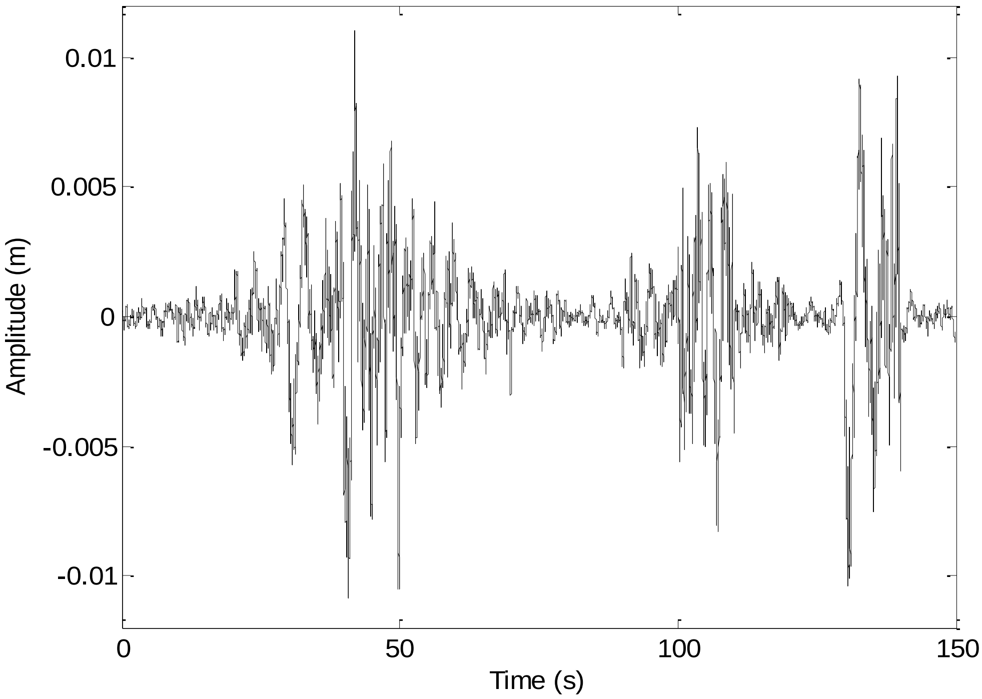

Fig. 7. Road profile for test with varying road class.

From Fig. 8, the BS method again outperformed the FT, LS, KF and KB methods in tracking the changes in the road profiles. The percentages of correct classification are 43.3% for FT, 23.0% for LS, 60.0% for KF, 61.0% for KB and 84.0% for BS. The percentages where a road segment was incorrectly classified more than one class away are 27.0% for FT, 45.7% for LS, 0.67% for KF, 6.00% for KB and 0.33% for BS. Interestingly, no particular deterioration in the accuracy was observed immediately after a change in the road class. Since the BS technique gives the highest accuracy and the lowest number of cases where a road segment was incorrectly classified more than one class away, this shows that the proposed classification using the BS method is very much feasible in the practical scenario where there may be several changes in the road class throughout a journey.

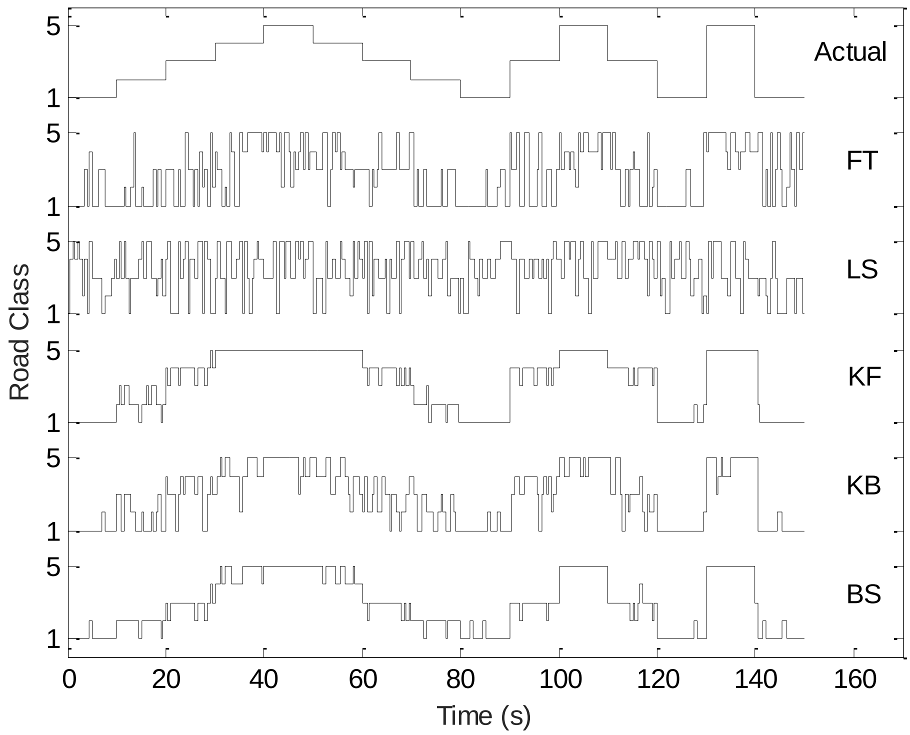

Fig. 8. Road class estimated by various methods at 18km/hr (5ms^{-1}). Road Classes A, B, C, D and E are represented by the level values 1, 2, 3, 4 and 5, respectively.

4.4 Performance Comparison at Higher Velocity

Experiments were repeated at a higher velocity of 72km/hr (20ms^{-1}). Only road profiles A, B and C could be tested due to the responses for road profiles D and E exceeding hardware limitations. Results of the accuracy of road classification are shown in Table 2; these were obtained in a similar way as those in Table 1. The percentages of correct classification across all three road profiles are 49.1% for FT, 39.0% for LS, 64.0% for KF, 67.4% for KB and 91.6% for BS. An improvement is observed for all techniques except the FT technique, when compared with the results obtained at 18km/hr (5ms^{-1}). This is likely attributed to the smaller number of classes from which the classification was performed. The superiority of the BS method is again evident. Note that this is achieved without any retuning of the hyperparameters of the TC kernel.

Table 2. Classification results for various methods at 72km/hr (20ms^{-1}). The bold values indicate correct classification.

Actual road class	Method	Number of occurrences of estimated road class		
		A	B	C
A	FT	**340**	203	47
	LS	**196**	96	298
	KF	**454**	136	0
	KB	**369**	207	14
	BS	**590**	0	0
B	FT	185	**290**	115
	LS	144	**192**	254
	KF	0	**89**	501
	KB	42	**377**	171
	BS	7	**581**	2
C	FT	57	294	**239**
	LS	124	163	**303**
	KF	0	0	**590**
	KB	4	139	**447**
	BS	29	111	**450**

A final experiment was conducted using a road profile with varying road class. The results are shown in Fig. 9. The percentages of correct classification are 49.3% for FT, 38.6% for LS, 64.3% for KF, 69.3% for KB and 95.0% for BS. The BS method outperformed all four competing techniques, thus showing its potential impact to the vehicle suspension community.

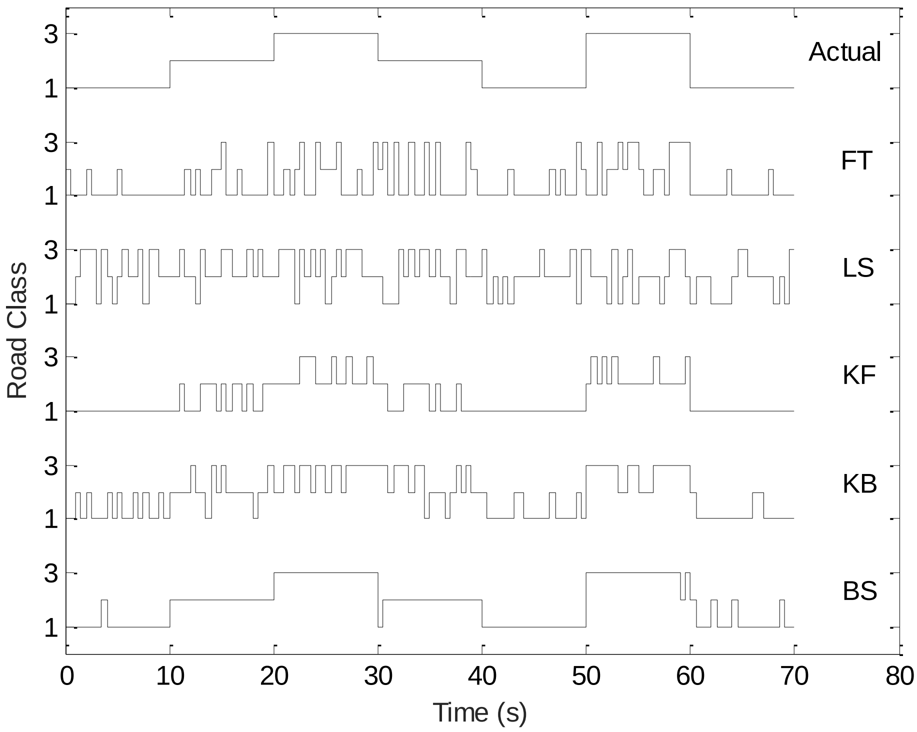

Fig. 9. Road class estimated by various methods at 72km/hr (20ms^{-1}). Road Classes A, B and C are represented by the level values 1, 2 and 3, respectively.

5. Conclusions

The BS method was proposed for classifying road roughness according to the ISO road classification. The method is based on Bayesian regression for the estimation of impulse responses. The FRM patterns corresponding to these impulse responses are utilized for classification. High accuracy can be achieved due to the incorporation of the prior dc gain into the BS formulation. The proposed technique remains effective without any recalibration when the load carried by the vehicle changes and can deal with varying vehicle velocity in a straightforward manner. Experiments on a laboratory-scale system attained drastic improvements in the classification accuracy in both the scenarios of passive and active suspensions, using a detection time of 0.5s and a training time of 5s for each road class. The proposed approach thus offers a low-cost, model-free and fast solution to the problem of road classification, which is feasible for practical implementation. Suggestions for future work include applying the proposed method to roads with different waviness as well as enhancing controller design based on the estimated road class.

References

[1] T. Saarenketo, T. Scullion, Road evaluation with ground penetrating radar, J. Appl. Geophysics 43 (2000) 119–138. https://doi.org/10.1016/S0926-9851(99)00052-X.

[2] Standard Test Method for Measuring Pavement Roughness Using a Profilograph, ASTM Standard E1274, 2018.

[3] F. Kilic, J. Hilsmann, Application and improvement of the TRRL (Transport and Road Research Laboratory) high-speed laser profilometer algorithm with sensor fusion, IFAC-PapersOnLine 49 (2016) 260–265. https://doi.org/10.1016/j.ifacol.2016.07.761.

[4] K.-S. Hong, H.-C. Sohn, J.K. Hedrick, Modified skyhook control of semi-active suspensions: A new model, gain scheduling, and hardware-in-the-loop tuning, J. Dyn. Syst. – T. ASME 124 (2002) 158–167. https://doi.org/10.1115/1.1434265.

[5] A. González, E.J. O’brien, Y.-Y. Li, K. Cashell, The use of vehicle acceleration measurements to estimate road roughness, Vehicle Syst. Dyn. 46 (2008) 483–499. https://doi.org/10.1080/00423110701485050.

[6] S. Wang, S. Kodagoda, L. Shi, H. Wang, Road-terrain classification for land vehicles: Employing an acceleration-based approach, IEEE Veh. Technol. Mag. 12 (2017) 34–41. https://doi.org/10.1109/MVT.2017.2656949.

[7] N.K. Harris, A. Gonzalez, E.J. Obrien, P. McGetrick, Characterisation of pavement profile heights using accelerometer readings and a combinatorial optimisation technique, J. Sound Vib. 329 (2010) 497–508. https://doi.org/10.1016/j.jsv.2009.09.035.

[8] Y. Qin, C. Xiang, Z. Wang, M. Dong, Road excitation classification for semi-active suspension system based on system response, J. Vib. Control 24 (2017) 2732–2748. https://doi.org/10.1177/1077546317693432.

[9] Y. Qin, R. Langari, Z. Wang, C. Xiang, M. Dong, Road excitation classification for semi-active suspension system with deep neural networks, J. Intell. Fuzzy Syst. 33 (2017) 1907–1918. https://doi.org/10.3233/JIFS-161860.

[10] J.J. Rath, K.C. Veluvolu, M. Defoort, Simultaneous estimation of road profile and tire road friction for automotive vehicle, IEEE T. Veh. Technol. 64 (2015) 4461–4471. https://doi.org/10.1109/TVT.2014.2373434.

[11] S.-W. Kang, J.-S. Kim, G.-W. Kim, Road roughness estimation based on discrete Kalman filter with unknown input, Vehicle Syst. Dyn. 57 (2019) 1530–1544. https://doi.org/10.1080/00423114.2018.1524151.

[12] G.-W. Kim, S.-W. Kang, J.-S. Kim, J.-S. Oh, Simultaneous estimation of state and unknown road roughness input for vehicle suspension control system based on discrete Kalman filter, Proc. Inst. Mech. Eng. D. – J. Automobile Eng. 234 (2020) 1610–1622. https://doi.org/10.1177/0954407019894809.

[13] W. Fauriat, C. Mattrand, N. Gayton, A. Beakou, T. Cembrzynski, Estimation of road profile variability from measured vehicle responses, Vehicle Syst. Dyn. 54 (2016) 585–605. https://doi.org/10.1080/00423114.2016.1145243.

[14] A.H. Tan, D.S. Ong, Kernel-based impulse response estimation with prior DC gain using built-in self-scaling technique, IEEE T. Instrum. Meas. 69 (2020) 7295–7305. https://doi.org/10.1109/TIM.2020.2975528.

[15] C.E. Rasmussen, C.K.I. Williams, Gaussian Processes for Machine Learning, MIT Press, USA, 2006.

[16] M. Haddar, S.C. Baslamisli, R. Chaari, F. Chaari, M. Haddar, Road profile identification with an algebraic estimator, J. Mech. Eng. Sci. 233 (2019) 1139–1155. https://doi.org/10.1177/0954406218767470.

[17] C. Poussot-Vassal, O. Sename, L. Dugard, P. Gáspár, Z. Szabó, J. Bokor, A new semi-active suspension control strategy through LPV technique, Control Eng. Pract. 16 (2008) 1519–1534. https://doi.org/10.1016/j.conengprac.2008.05.002.

[18] M.M. Morato, M.Q. Nguyen, O. Sename, L. Dugard, Design of a fast real-time LPV model predictive control system for semi-active suspension control of a full vehicle, J. Frankl. Inst. 356 (2019) 1196–1224. https://doi.org/10.1016/j.jfranklin.2018.11.016.

[19] P. Gaspar, Z. Szabo, J. Bokor, Estimating road roughness by using a linear parameter varying model, IFAC Proc. Vol. 36 (2003) 103–108. https://doi.org/10.1016/S1474-6670(17)35647-1.

[20] J.M. Palma, C.F. Morais, R.C.L.F. Oliveira, H_2 control and filtering of discrete-time LPV systems exploring statistical information of the time-varying parameters, J. Frankl. Inst. 357 (2020) 3835–3864. https://doi.org/10.1016/j.jfranklin.2020.02.029.

[21] Mechanical Vibrations – Road Surface Profiles – Reporting of Measured Data, second ed., ISO 8608, 2016.

[22] P. Múčka, Simulated road profiles according to ISO 8608 in vibration analysis, J. Test. Evaluation 46 (2018) 405–418. https://doi.org/10.1520/JTE20160265.

[23] Y. Fujimoto, T. Sugie, Kernel-based impulse response estimation with a priori knowledge of the DC gain, IEEE Control Syst. Lett. 2 (2018) 713–718. https://doi.org/10.1109/LCSYS.2018.2847415.

[24] A.F. Jahromi, A. Zabihollah, Linear quadratic regulator and fuzzy controller application in full-car model of suspension system with magnetorheological shock absorber, Proc. 2010 IEEE/ASME Int. Conf. Mechatron. Embedded Syst. Appl., Qingdao, China, 2010, 522–528. https://doi.org/10.1109/MESA.2010.5552010.

[25] H. Liu, K. Nonami, T. Hagiwara, Semi-active fuzzy sliding mode control of full vehicle and suspensions, J. Vib. Control 11 (2005) 1025–1042. https://doi.org/10.1177/1077546305053399.

[26] M. Rezaee, V. Shaterian-Alghalandis, A. Banan-Nojavani, Development of the smooth orthogonal decomposition method to derive the modal parameters of vehicle suspension system, J. Sound Vib. 332 (2013) 1829–1842. https://doi.org/10.1016/j.jsv.2012.11.007.

[27] T. Chen, H. Ohlsson, L. Ljung, On the estimation of transfer functions, regularizations and Gaussian processes – Revisited, Automatica 48 (2012) 1525–1535. https://doi.org/10.1016/j.automatica.2012.05.026.

[28] J.S. Maritz, T. Lwin, Empirical Bayes Methods with Applications, second ed., CRC Press, USA, 2017.

[29] A.H. Tan, Linear approximation of bilinear processes, IEEE T. Control Syst. Technol. 13 (2005) 224 – 232. https://doi.org/10.1109/TCST.2004.839557.

[30] T. Chen, On kernel design for regularized LTI system identification, Automatica 90 (2018) 109–122. https://doi.org/10.1016/j.automatica.2017.12.039.

[31] Y. Qin, Z. Wang, C. Xiang, E. Hashemi, A. Khajepour, Y. Huang, Speed independent road classification strategy based on vehicle response: Theory and experimental validation, Mech. Syst. Signal Process. 117 (2019) 653–666. https://doi.org/10.1016/j.ymssp.2018.07.035.

[32] Quanser, Active Suspension System: User Manual, Quanser Corporation, 2013.

[33] J.Y. Wong, Theory of Ground Vehicles, third ed., John Wiley & Sons, Inc., USA, 2001.

[34] A.H. Tan, Multi-input identification using uncorrelated signals and its application to dual-stage hard disk drives, IEEE T. Magn. 54 (2018) Article No. 9300604. https://doi.org/10.1109/TMAG.2018.2856209.

[35] A.H. Tan, K.R. Godfrey, Industrial Process Identification: Perturbation Signal Design and Applications, first ed., Springer, Switzerland, 2019.